Journal of the Serbian Chemical Society
JSCS-info@shd.org.rs • www.shd.org.rs/JSCS
J. Serb. Chem. Soc. 81 (9) 1055–1068 (2016) UDC 678:66.014+544.526:542.952.6:547.631.6
JSCS–4907 *Original scientific paper*

Polymer–graphene composites by the photocuring of a system containing benzophenone macromer

FLORENTINA JITARU[1], ANDREEA L. CHIBAC[1], GEORGE EPURESCU[2], IOANA ION[3] and TINCA BURUIANA[1]*

[1]*Petru Poni Institute of Macromolecular Chemistry, 41 A Grigore Ghica Voda Alley, 700487 Iasi, Romania,* [2]*National Institute for Lasers, Plasma and Radiation Physics, Atomistilor 409, 077125 Bucharest-Magurele, Romania and* [3]*National Institute for Research and Development in Electrical Engineering ICPE-CA, Splaiul Unirii.313, Sector 3, Bucharest, Romania*

(Received 18 December 2015, revised 7 April, accepted, 11 April 2016)

Abstract: Formulations incorporating benzophenone–oligodimethacrylate (BP–DMA) and graphene structures, *i.e.*, graphene oxide (GO) and reduced graphene oxide (RGO), were exposed to UV–Vis irradiation or a femtosecond laser beam to achieve hybrid composites. All structures were characterized through various methods, including ^{1}H-NMR and FTIR spectroscopies, optical microscopy, TEM, ESEM/EDAX analysis and DSC/XRD techniques. The photopolymerization of BP–DMA in the monomer compositions with and without GO or RGO was investigated by photo-DSC and FTIR methods to determine the kinetic parameters of the polymerization. The photopolymerization experiments revealed a good photoreactivity of the monomers (degree of conversion: 65–77 %) after 1 min exposure to UV–Vis irradiation and the addition of graphene (up to 0.5 %), whereas the polymerization rate varied between 0.14 and 0.1 s^{-1}. Moreover, two-photon photopolymerization of the formulations in the presence/absence of GO or RGO nanosheets (0.1 wt. %) generated 2D microstructures by the direct laser writing procedure. Furthermore, the morphology and the properties of composites materials were analyzed.

Keywords: graphene–polymer composites; photocuring; two photon polymerization; benzophenone macromer.

INTRODUCTION

In modern research, the field of nanoscience plays a crucial role in the blossoming future of nanotechnology, especially in areas such as computing, sensors, photonics, biomedical and other applications. In this vision, the discovery of graphene[1] and graphene–polymer composites open new horizons in the achievement of multifunctional materials with advanced performance[2–5] compared with

* Corresponding author. E-mail: tbur@icmpp.ro
doi: 10.2298/JSC151218040J

those exhibited by polymers. Thus, graphene–polymer composites show improved thermal, mechanical, gas barrier, electrical and flame retardant properties,[6–9] for which reasons they have found applications in the areas of electronics, sensors, solar cells, memory devices, anti-static coatings and biomedical engineering.[10–14] However, the physicochemical properties of such materials depend on the distribution of graphene layers inside the polymer composite and the control of interfacial linkage between the filler and the organic matrix. As reported, pristine graphene is not able to form homogeneous composites due to its incompatibility with the organic component, while graphene oxide sheets are friendlier with the organic phase,[15,16] and this feature recommends GO as nanofiller for hybrid composites. On the other hand, GO is electrically insulating, and RGO is suitable for obtaining conducting nanocomposites. In the literature, there are a variety of strategies for the development of polymer–graphene nanocomposites, including non-covalent dispersion and covalent attachment of the polymer to filler. These techniques allowed the design of new hybrid materials using different organic templates, such as epoxy resins, poly(methyl methacrylate), poly(vinyl alcohol), polystyrene, polyimides, polyurethanes and others.[10,15]

Among the procedures employed to achieve hybrid nanocomposites, UV--curing methods proved to be useful in the production of coatings, dental materials, adhesives, stereolithography, *etc*.[17–19] The fast conversion of the liquid monomers in the absence of solvent led to a great variety of materials with tailored physicochemical and mechanical properties. The most suitable monomers are the (meth)acrylates, the reactivities of which depend on their chemical structure, the distance and flexibility between functional units, viscosity and hydrogen bonding.[20–22] Additionally, two-photon polymerization (2PP) induced with femtosecond laser pulses offers the possibility to create 2D/3D (micro)-nanostructures with complicated geometry.[23,24] To date, there are some photosensitive hybrids of the sol–gel type,[25,26] which were tested for microscale fabrication technology by 2PP.[27,28] Hence, several groups have investigated the photonic/optoelectronic characteristics of graphene derivatives,[29,30] and described the fabrication of 2D and 3D architectures using graphene–polymer composites.[31]

In this paper, the properties are reported of some hybrid composites prepared using a novel benzophenone oligodimethacrylate (BP–DMA) and carbonic filler using different techniques of photopolymerization, including UV–Vis irradiation and laser beam curing. The choice of BP–DMA besides other urethane macromers with different functionalities was motivated by the good-film forming properties of these combinations and the quality of the benzophenone dimethacrylate to act as type II macromolecular photoinitiator for UV-curable resins. Actually, the concept of macroinitiators incorporating photosensitive groups is considered a viable alternative for their application in photocrosslinkable systems with

higher efficiency.[32] Other advantage of acid macromers is that these provide additional hydrogen bonding sites that may enhance the physical–mechanical properties of the final materials, but this aspect will be described in a future paper. The influence of graphene oxide and reduced graphene oxide on the conversion and the rate of polymerization in the case of two formulations exposed to irradiation were studied, together with the synthesis of materials by 2PP polymerization in presence of small quantities of GO/RGO.

EXPERIMENTAL

Materials

Benzophenone-3,3′,4,4′-tetracarboxylic acid dianhydride, 1,6-diisocyanato-2,2,4-trimethylhexane, 2-hydroxyethyl methacrylate (HEMA), poly(propylene oxide) diol (PPO, $\bar{M}_w$ = = 2000 g mol^{-1}), 2-isocyanatoethyl methacrylate, poly(ethylene oxide) (PEG, $\bar{M}_w$ = 1000 g mol^{-1}), polytetrahydrofuran (PTHF, $\bar{M}_w$ = 1000 g mol^{-1}), isophorone diisocyanate and 2,2-bis(hydroxymethyl)propionic acid (DMPA) were purchased from Sigma–Aldrich and used without further purification. The initiator was 2-benzyl-2(dimethylamino)-1-[4-(morpholin-4-yl)phenyl]butan-1-one (Irgacure 369) from Ciba and graphite powder from Oltchim-Ramnicu Valcea, Romania (<600 μm, with 99.9 % C).

Equipment

The structure of compounds was verified by ^{1}H-NMR and FTIR spectroscopy (the data are given in Supplementary material to this paper). The ^{1}H-NMR spectra were recorded on a Bruker 400 MHz spectrometer in $CDCl_3$ at room temperature, whereas the FTIR spectra using a Specord M80. For FTIR kinetics, the samples were exposed to UV–Vis irradiation using a LA 500 device (λ = 400–500 nm, intensity of light, 2.5–3.0 mW cm^{-2}) at room temperature. The morphology of the films was investigated using optical microscopy (Leica DM2500 M), environmental scanning electron microscope Quanta200 coupled with an energy dispersive X-ray spectroscope (ESEM/EDAX) and TEM measurements (Hitachi High-Tech HT7700 microscope with an accelerating voltage of 100 kV). The photocalorimeter (DPC 930, TA Instruments from DuPont) consisted of a differential calorimeter scanning device with a UV light source mounted on the top. A standard 200 W super high-pressure mercury arc lamp was used as the light source. The intensity of the light in the sample compartment was of 5 mW cm^{-2}. Typically, 1.5–2.0 mg of the monomer mixture with the photoinitiator was placed in an aluminum DPC pan. A poly(ethylene terephthalate) (Mylar® film) was used to cover the liquid in the photo-DSC pan, to prevent atmospheric oxygen from diffusing into the sample. The polymerizations were performed under an air atmosphere. Viscosity measurement for the formulations was performed with a Dial Reading Brookfield viscometer at 25.0±0.2 °C, in triplicate. The test was run with a RV/HA/HB-7 spindle, at spindle speeds of 6 and 12 rpm, and the viscosity readings obtained were recorded and expressed as Pascal second (Pa s). The thermal transitions were measured on a Mettler DSC 1 STARe device by cooling of the materials to –100 °C and heating at a rate of 10 °C min^{-1} up to 250 °C. X-ray patterns were recorded with a D8 Advance Bruker AXS diffractometer and the difractograms were studied with EVA software (from DIFFRAC Plus evaluation package). The X-rays were generated using a CuK_α (λ = 0.1541 nm) source with an emission current of 40 mA and a voltage of 36 kV. The diffractograms were recorded in the 2θ range 10 to 80° at room temperature at a scan rate of 5° min^{-1}. The set-up for the 2PP experiments is a self-made direct laser writing (DLW) workstation coupled with a Clark CPA-2010 amplified femtosecond laser working at a wave-

length of 775 nm, having pulse duration of 200 fs and a repetition rate of 2 kHz. The viscous monomer mixtures containing few drops of tetrahydrofuran as solvent were placed on an XYZ motion stage with stepper motors and piezodriver. The laser beam was moved on the sample using galvanic mirrors. A Z translation stage and a visualization system with CCD camera were used for precisely positioning the sample in the plane of the focused laser. Finally, the polymerized samples were washed with 2-propanol.

^{1}H-NMR data for BP–DMA, PPO–DMA and PEG–DMA are given in Supplementary material to this paper.

Preparation of graphene oxide (GO) and reduced graphene oxide (RGO)

GO and RGO were obtained by a modified Hummer–Offeman method, and from GO by thermal treatment at 1000 °C, respectively, from graphite powder.[33]

Synthesis of macromers

For the synthesis of benzophenone macromer (BP–DMA), PTHF macrodiol was used together with benzophenone-3,3′,4,4′-tetracarboxylic acid dianhydride (BP), 1,6-diisocyanato--2,2,4-trimethylhexane (TMDI) and 2-hydroxyethyl methacrylate (HEMA), employing the following PTHF:BP:TMDI:HEMA mole ratio: 2:1:2:2. Thus, 5 g PTHF (5 mmol) were degassed in vacuum for 2 h (100 °C) and then the temperature was reduced to 65 °C, when 10 mL DMF solution containing 0.85 g (2.5 mmol) BP were added and the mixture was stirred at 65 °C for 8 h in presence of pyridine as catalyst. After removal of the solvent, the product was dissolved in CH_2Cl_2 and the organic phase was washed with saturated aqueous solution of NaCl. After removal of the solvent under reduced pressure, 2.5 mmol of product were dissolved in 10 mL THF, and then 1.05 mL (5 mmol) TMDI were added to the reaction mixture in the presence of dibutyltin dilaurate as catalyst. The mixture was kept under stirring at 40° C for 24 h and finally, 0.62 ml (5 mmol) of HEMA was added and the mixture stirred for 10 h. The course of the reaction was pursued through the infrared absorption of the isocyanate stretching band at 2260 cm^{-1}; the reaction being considered complete after the disappearance of this band from the FTIR spectrum. After evaporation of the solvent under reduced pressure, the BP–DMA was collected as a pale yellow viscous liquid.

Similarly, the macromer PPO–DMA was prepared starting from poly(propylene oxide) diol ($\bar{M}_w$ = 2000 g mol^{-1}) and 2-isocyanatoethyl methacrylate.[34] The carboxylic macromer (PEG–DMA) was also obtained using poly(ethylene oxide) (PEO, $\bar{M}_w$ = 1000 g mol^{-1}), isophorone diisocyanate, 2,2-bis(hydroxymethyl)propionic acid (DMPA) and 2-hydroxyethyl methacrylate (HEMA) taken in a mole ratio of 0.5:2:0.5:2.[35]

Photopolymerization

The monomer mixtures based on BP–DMA/PPO–DMA or BP–DMA/PEG–DMA and Irgacure 369 (3 %) were homogenized and coated manually on the Teflon plates (2.5 cm×2.5 cm) to be irradiated with UV–Vis light up to the formation of polymer networks (Table I). The preparation of hybrid composites needed the incorporation of GO/RGO in each formulation, which then was subjected to irradiation.

TABLE I. Photo-DSC data of formulations F1 (15 % BP–DMA/85 % PPO–DMA) and F2 (15 % BP–DMA/85 % PEG–DMA); DC – degree of conversion

Sample	*DC* by photo-DSC, %	*DC* by FTIR, %	t_{max} / s	R_{pmax} / 10^{-2} s^{-1}
F1	74	81	3.0	13.7
F1 + 0.5 % GO	72	80	4.0	11.5

TABLE I. Continued

Sample	*DC* by photo-DSC, %	*DC* by FTIR, %	t_{max} / s	R_{pmax} / 10^{-2} s^{-1}
F1 + 0.5 % RGO	72	77	4.0	11.0
F2	77	86	3.0	14.0
F2 + 0.01 % GO	75	86	3.5	11.0
F2 + 0.1 % GO	73	85	3.5	11.0
F2 + 0.5 % GO	67	72	4.0	10.0
F2 + 0.1 % RGO	74	85	3.5	12.0
F2 + 0.5 % RGO	65	73	3.5	11.5

RESULTS AND DISCUSSION

Characterization of the inorganic filler

The morphology and structure of the graphene oxide (GO) and reduced graphene oxide (RGO) used in this study were investigated through FTIR spectroscopy and TEM observation. The FTIR spectrum of GO, shown in Fig. 1, revealed the presence of different types of oxygen functionalities with specific bands corresponding to the O–H stretching vibrations (3432 cm^{-1}), stretching vibrations from C=O (1724 cm^{-1}), skeletal vibrations from non-oxidized graphitic domains (1621 cm^{-1}), C–OH stretching vibrations (1273 cm^{-1}), and the C–O unit absorption (1050 cm^{-1}). In case of the RGO, it can be noted that the O–H vibration band at 3432 cm^{-1} was slightly diminished, while the stretching vibrations from C=O at 1724 cm^{-1} were appreciably reduced due to the deoxygenation process. However, the specific band from 1050 cm^{-1} could still be identified owing to the carboxyl groups present even after thermal treatment.

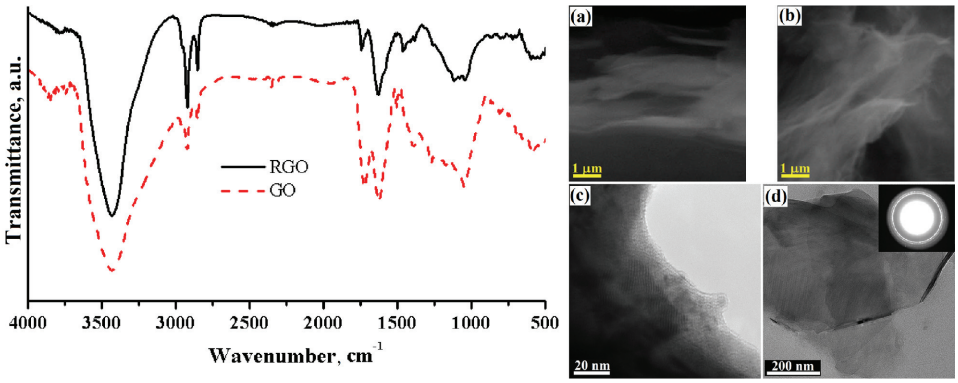

Fig. 1. FTIR spectra of graphene oxide (GO) and reduced graphene oxide (RGO); TEM images of graphene oxide GO (a and c) and reduced graphene oxide RGO (b and d).

The TEM images corresponding to GO and RGO displayed a curled and restacked morphology among sheets, monolithic sheets, and wavy structures.[36,37] The micrographs of GO (Fig. 1a and c) confirmed the flat structure of the nano-

sheet, which appeared through the ultrasonication process during sample preparation as result of the destroyed van der Waals interactions between the GO layers. On the other hand, the RGO nanosheets are layer structured, irregular and folding, as observed in Fig. 1b and d. Such processes suggest the intrinsic nature of graphene, in which the 2D membrane structure is thermodynamically more stable *via* blending.[38] In addition, the selected image (inset, Fig. 1d) showed the hollow diffraction rings of material suggesting an amorphous nature of the RGO structures.

Photopolymerization study

As the aim of this work was the preparation of graphene–polymer composites based on the methacrylic structures given in Scheme 1, first the photopolymerization kinetics of the formulations containing a benzophenone oligodimethacrylate (BP–DMA) and the other urethane co-monomer (PPO–DMA, PEG–DMA) were evaluated using the photo-DSC technique and FTIR analysis.

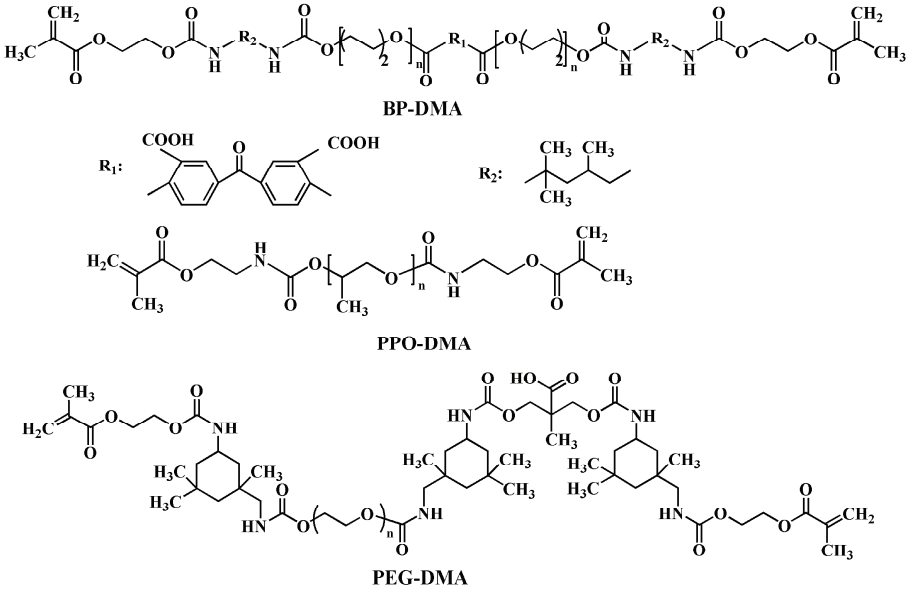

Scheme 1. Structures of the difunctional monomers used in the photopolymerization studies.

Consequently, the double bond conversion (*DC*) to single bonds after polymerization of the macromers under UV light irradiation, the photopolymerization rate (R_p), and the time to attains the maximum polymerization heat (t_{max}) were determined at room temperature in the presence/absence of GO or RGO. Typical plots of the double bond conversion and the polymerization rate *versus* UV irradiation time are displayed in Fig. 2 for two formulations incorporating 15 wt. % benzophenone dimethacrylate (BP–DMA) and 85 wt.% PPO–DMA (F1)

or PEG–DMA (F2) macromers. Photopolymerization experiments performed in presence of Irgacure 369 showed that in F1 and F2 (Table I), the conversion values were of 74 (F1, after 23 s of UV irradiation) and 77 % (F2, after 18 s), respectively, whereas the polymerization rate was similar for both formulations (F1: 13.7×10^{-2} s^{-1}; F2: 14×10^{-2} s^{-1}). At this point, it should be remembered that the photopolymerization of urethane dimethacrylates is initiated by free radicals generated *via* UV irradiation of the benzophenone unit from BP–DMA in presence of Irgacure 369. Actually, the synergistic effect of the benzophenone macromer in free radical copolymerizations using Irgacure as co-initiator was reported earlier.[39]

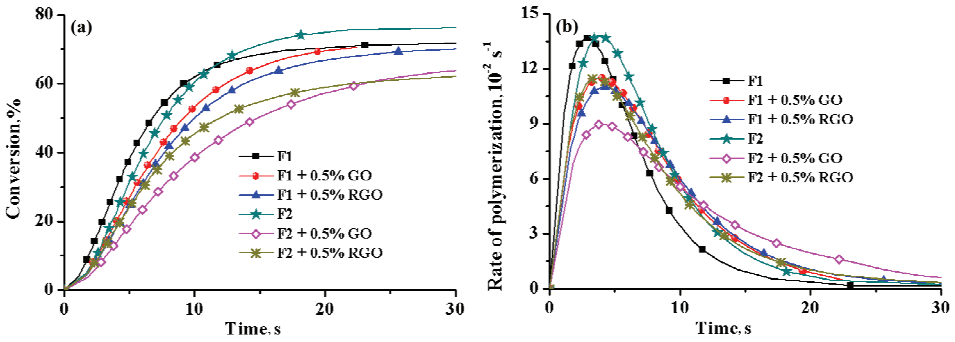

Fig. 2. Double bond conversion (a) and polymerization rate, R_p (b), as a function of irradiation time for formulations based on BP–DMA in the presence of 3 wt. % Irgacure 369.

In order to evaluate the effect of GO or RGO on the photobehavior of the monomers, the double bond conversion and the polymerization rate were calculated, the filler loading was varied from 0.01 up to 0.5 wt. %. Hence, the addition of 0.5 % GO or RGO inside F1 did not notably influence the final double bond conversion, but affected slightly the rate of polymerization, this being reduced by about 20 %. No significant difference was found for the kinetic parameters of the F2 formulation with 0.01 wt. % GO, in agreement with the results reported by Sangermano *et al*. on the UV curing of a poly(ethylene glycol) diacrylate/GO/ /water dispersion.[40] An increase of the GO or RGO amount to 0.5 wt. % in the macromer mixture decreased the double bond conversion to 67 and 65 %, respectively (F2+0.5 wt. % filler). A similar response was identified in the maximum polymerization rate, when R_{pmax} decreased from 0.14 to 0.11 s^{-1} for 0.5 wt. % RGO loading (Fig. 2). The lower rate of polymerization could be explained by the restricted mobility of the reactive species, which reduced the crosslinking density, facilitating termination and, presumably, the UV shielding effect of graphene, as reported for epoxy resins.[41]

This trend was confirmed by the FTIR spectroscopy, where a gradual decrease of the vibration of the double bond centered at 816 cm^{-1} with increasing

irradiation time was evidenced. The changes in the FTIR spectra profile of the formulation F2 with irradiation time, reflected through a double bond conversion of 86 % after 150 s of exposure to UV–Vis light are illustrated in Fig. 3a. As can be seen from the data given in Table I, this value was higher compared to F1, for which the conversion degree was 81 %. Additionally, the soluble fraction of the cured films was estimated by extracting the films with $CHCl_3$ for 24 h and low values of 6 (F1) and 7 % (F2), respectively, were obtained due to post-curing. Furthermore, the addition of graphene to the photopolymerizable composition caused a diminution of both the polymerization rate and the final conversion as a function of the filler loading. The relations between the exposure time and the degree of conversion of methacrylate units in the formulations F1 and F2 with and without GO/RGO in different amounts are shown in Fig. 3b. From the kinetic plots, the double bond conversion varied between 72 (F2 + 0.5 wt. % GO) and 86 % (F2 + 0.01 wt. % GO) depending on the amount of filler, without neglecting the viscosity of the uncured systems (F1: 4.5 Pa s; F2: 12.7 Pa s) and the diffusion-controlled reactions (propagation and termination) as the photopolymerization proceeded.

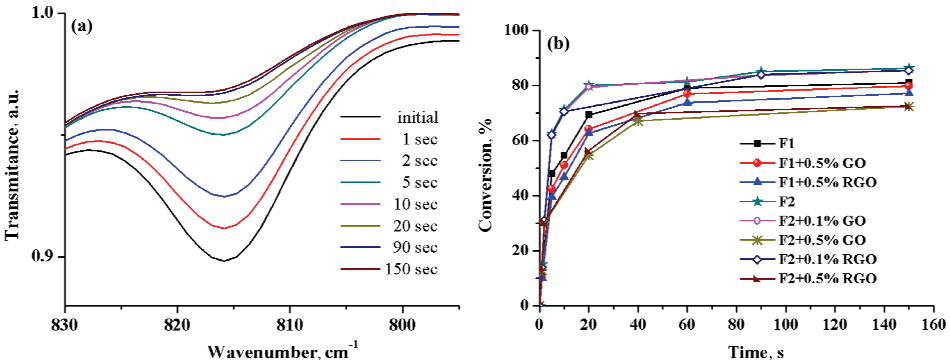

Fig. 3. Changes in the FTIR spectrum: a) for the absorption band of double bonds in the formulation F2 upon UV–Vis exposure and b) changes in the conversion with irradiation time for all formulations.

Morphological investigation

Next, the crystal structure and morphological aspects of GO or RGO graphene nanosheets and their polymeric composites were examined using X-ray diffraction, ESEM/EDX and TEM analyses. The XRD patterns of pristine GO and RGO nanosheets together with that for the F2 hybrid formulation are presented in Fig. 4a. The disappearance of the native graphite peak at 2θ 26.7° (attributed to a d-spacing of 0.33 nm) and the appearance of sharp peak centered at 2θ 12.4° in the diffractogram of GO are proof of the successful oxidation of the starting graphite. The peak assigned to graphene oxide indicates an interlayer

spacing of 0.72 nm, which confirms the existence of oxygen functionalities capable of facilitating the hydration and exfoliation of GO structures into an aqueous medium. This result can be related to the (001) reflection peak, which might depend on the method of preparation as well as the number of layers in the gallery space of the material.[42] After thermal treatment, all peaks disappeared and the XRD spectrum shows a wide diffraction peak at 26.5° corresponding to a *d*-spacing of 0.34 nm. In addition, using the Scherrer equation,[43] the crystalline size (or thickness) of the (002) was estimated to be 30.1 Å, corresponding to approximately three layers (thickness/d_{002}). The XRD data for GO and RGO indicated that the filler preserved the graphitic structure. In the case of XRD profiles of the composite films based on F2 with 0.5 % GO or RGO, the peak of GO stacking disappeared, suggesting a certain amount of disorder and loss of structural regularity of the graphene. Thus, GO and RGO in each film were exfoliated and dispersed at the molecular level into the photopolymerized matrix.[44]

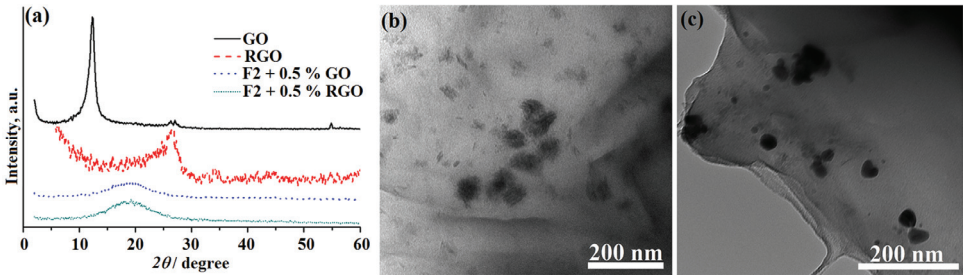

Fig. 4. a) XRD patterns for GO/RGO and the composites based on F2 formulation with 0.5 % GO or RGO loading, and TEM images for: b) F2+0.5 % GO and c) F2+0.5 % RGO.

The TEM image for F2 with 0.5 % GO (Fig. 4b) confirms that GO was exfoliated from the polymer matrix, producing GO sheets with dimensions under 100 nm, but, unfortunately, they have a tendency to agglomerate forming larger GO structures. This observation suggests that there were no strong interactions between the carboxylic groups of the urethane–acrylic network and the functionalities present in the graphene nanosheets. The TEM image of F2 with 0.5 % RGO loading (Fig. 4c) displayed the same exfoliated structure of RGO in the organic phase. The morphology of the photopolymerized materials was also investigated by ESEM/EDAX using cross sections of the polymeric films (Fig. S-1 of the Supplementary material). Note that the photograph of the polymer film indicated the appearance of microphase separation of the soft (PEO, PTHF) and hard (urethane) components from the resulting poly(urethane–acrylate) network and the existence of microparticles assigned probably to the hard segments. From the analysis of the F2 formulation, typical elements were found in the mixtures, namely C, N, O with atomic percentages of 78, 7.24 and 14.78 %, respectively. For hybrids derived from the F2 with 0.5 GO (C: 74.14 %; N: 8.86 %; O: 17.00

%) or RGO (C: 82.00 %; N: 4.87 %; O: 13.18 %) in composition, the EDAX spectra showed the same elements as in the F2 organic matrix, but the atom ratios were a function of the amount of added filler.

Thermal characterization

The thermal characteristics of the uncured macromers (BP–DMA, PEG–DMA) and the film containing BP–DMA/PEG–DMA (F2 formulation) were studied by differential scanning calorimetry (DSC) in order to observe the changes that occurred when they were heated. In the DSC thermograms collected on the second heating, the macromer BP–DMA showed one peak at around –65.41 °C, which could be associated with the glass transition temperature (T_g) of the polytetramethylene oxide used in its synthesis (Fig. 5) together with another two exothermic peaks at ~ –25 and 130.14 °C, which indicate the presence of some crystalline entities of PTHF and consummation of the reactive end groups (thermal cross-linking reaction), respectively. A further endothermic peak that appeared at 15.62 °C may be related to the melting temperature of the small amount of slightly ordered polyether phase. In the case of PEG–DMA, the T_g was identified at –37.57 °C and the exothermic peak at 137.21 °C (thermal crosslinking). In the DSC curve of the polymeric network F2, the T_g was found at –41.5 °C and the melting peak of the flexible segments at 17.2 °C. It can be noted that the melting temperatures of PTHF and PEO were reduced when they were present in the crosslinked network structure.

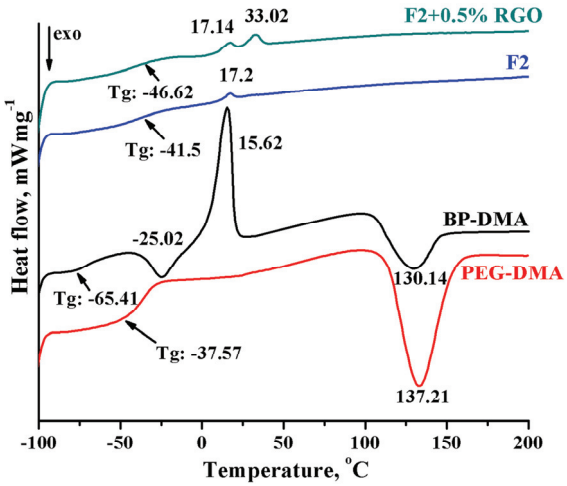

Fig. 5. DSC thermograms of the BP–DMA, PEG–DMA, and the F2 film with and without RGO filler.

The incorporation of graphene into the F2 with 0.5 % RGO gives rise to a slight diminution of the T_g (–46.6 °C), with the simultaneous appearance of two endothermic peaks (17.14 and 33 °C) caused probably by the folding and packing

of the long chain segments. The second endothermic peak may have originated from not fully cured polymers enclosed in the network.

Two-photon polymerization of methacrylic formulations

For the 2PP experiments, both formulations in the absence/presence of GO or RGO were used to build on glass substrates grids of 20×20 lines systems with a distance of 100 μm between lines. Optical microscopy (OM) images are presented in Fig. 6 (1, a–f) for grid microstructures processed at three laser powers (3.5, 7.5 and 10 mW).

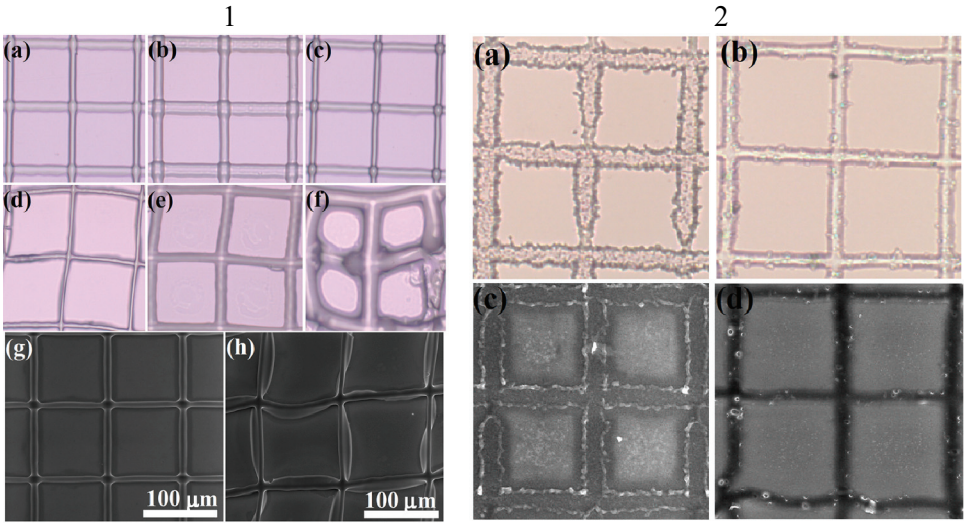

Fig. 6. 1 – Optical images of grids based on F1 and F2 formulations at different laser incident power: 3.5 (a, d); 7.5 (b, e) and 10 mW (c, f); SEM micrographs for materials based on F1 (g) and F2 (h) at a laser power of 3.5 mW; 2 – optical and SEM images of grids created of F2 +0.1 % GO (a, c) or RGO (b, d) at a laser incident power of 5 mW. The distance between the lines is 100 μm.

Starting from the formulation F1, the generation of well-defined structures with no influence of laser power and a good efficiency of the developing procedure was observed, the non-irradiated regions being completely cleaned. A comparable construction was processed for F2, but in this case, the yield of regular cured grids depended on the incident laser power. The thickness of the lines corresponding to the 2D structures varied from few μm up to 20 μm, and the SEM profiles (Fig. 6 (1, g and h) proved the formation of distinct grids from the above formulations without clear defects. Moreover, the photopolymerized lines corresponding to F2 could be detached from the substrate in order to create a freestanding scaffold. When the F2 formulation with 0.1 % GO or RGO was photopolymerized, the formed grids presented some imperfections in the

straightness of the lines (Fig. 6 (2)), which was probably due to the agglomerated GO/RGO nanosheets within the polymer matrix.

CONCLUSIONS

Two types of graphene nanofillers (GO and RGO) were introduced into photo-curable formulations based on photosensitive benzophenone oligodimethacrylate (BP–DMA) and other dimethacrylates used as co-monomers. The evaluation of photopolymerization behavior by photo-DSC and FTIR analysis demonstrated the UV shielding effect of graphene, for instance by adding 0.5 % graphene filler, the double bond conversion decreased by about 10 % compared to that for the pure formulation. ESEM and TEM images of the polymeric films suggested a good dispersion of GO/RGO sheets inside the organic matrix, where the exfoliated state of the carbonic components could be noticed. On the other hand, polymerization by a 2PP technique as a function of laser writing power led to 2D hybrid structures achieved by microstructuring of the formulations. The presence of the graphitic constituent in the photopolymerizable mixture allowed the formation of constructions with a few defects in the straightness of the lines. Thus, the photocuring of formulations in presence of graphene structures could be extended to prepare various hybrid materials with enhanced properties for technological applications in different fields.

SUPPLEMENTARY MATERIAL

^{1}H-NMR data for BP–DMA, PPO–DMA and PEG–DMA and SEM and EDAX analysis for the composites are available electronically at the pages of journal website: http://www.shd.org.rs/JSCS/, or from the corresponding author on request.

Acknowledgement. This work was supported by CNCSIS-UEFISCDI, Project No. PN-I--PT-PCCA-2011-3.1-1422.

ИЗВОД

ИЗРАДА ПОЛИМЕР–ГРАФЕН КОМПОЗИТА ФОТО-ПОЛИМЕРИЗАЦИЈОМ МАКРОМЕРА НА БАЗИ БЕНЗОФЕНОНА

FLORENTINA JITARU[1], ANDREEA L. CHIBAC[1], GEORGE EPURESCU[2], IOANA ION[3] и TINCA BURUIANA[1]

[1]Petru Poni Institute of Macromolecular Chemistry, 41 A Grigore Ghica Voda Alley, 700487 Iasi, Romania [2]National Institute for Lasers, Plasma and Radiation Physics, Atomistilor 409, 077125 Bucharest-Magurele, Romania и [3]National Institute for Research and Development in Electrical EngineeringICPE-CA, Splaiul Unirii no.313, sector 3, Bucharest, Romania

За израду хибридних полимер/графен композита примењена је фото-полимеризација олиго-диметакрилата (BP–DMA) на бази бензофенона и других диметакрилатних комономера у присуству графенских структура (графен-оксид/GO, редуковани графен-оксид/RGO) UV–Vis зрачењем или ласерским зрацима (импулс ласерског зрака 10–15 s). За карактеризацију добијених композита коришћене су различите методе, укључујући ^{1}H NMR и FTIR спектроскопију, оптичку микроскопију, TEM, SEM/EDAX и DSC/XRD анализу. Кинетички параметри реакције фото-полимеризације BP–DMA и комономера у присуству или без присуства GO или RGO су одређивани помоћу фото-DSC и FTIR.

Експерименти фотополимеризације су потврдили добру фото-реактивност одабраних мономера (степен конверзије: 65–77 %) након 1 минута излагања UV–Vis зрачењу и при додатку графена (до 0,5 mas.%), док је брзина полимеризације била у опсегу од 0,14 до 0,1 s^{-1}. Осим тога, двофотонска-фотополимеризација реакционе смеше у присуству/одсуству GO или RGO нанослојева (0,1 mas.%) је омогућила формирање 2Д микроструктуре применом методе директног ласерског писања. Такође су анализирана морфологија и својства хибридних композитних материјала.

(Примљено 18. децембра 2015, ревидирано 7. априла, прихваћено 11. априла 2016)

REFERENCES

1. K. S. Novoselov, A. K. Geim, S. V. Morozov, D. Jiang, Y. Zhang, S. V. Dubonos, I. V. Grigorieva, A. A. Firsov, *Science* **306** (2004) 666
2. A. K. Geim, *Science* **324** (2009) 1530
3. M. J. Allen, V. C. Tung, R. B. Kaner, *Chem. Rev*. **110** (2010) 132
4. Z. Sun, D. K. James, J. M. Tour, *J. Phys. Chem. Lett*. **2** (2011) 2425
5. F. Bonaccorso, Z. Sun, T. Hasan, A. C. Ferrari, *Nat. Photonics* **4** (2010) 611
6. C. N. R. Rao, A. K. Sood, *Graphene: Synthesis, Properties and Phenomena*, Wiley–VCH, Weinheim, 2013
7. Y. Xu, Y. Wang, L. Jiajie, Y. Huang, Y. Ma, X. Wan, Y. Chen, *Nano Res*. **2** (2009) 343
8. Y. R. Lee, A. V. Raghu, H. M. Jeong, B. K. Kim, *Macromol. Chem. Phys*. **210** (2009) 1247
9. D. Wang, X. Zhang, J. W. Zha, J. Zhao, Z. M. Dang, G. H. Hu, *Polymer* **54** (2013) 1916
10. J. Du, H. M. Cheng, *Macromol. Chem. Phys*. **213** (2012) 1060
11. G. L. Li, G. Liu, M. Li, D. Wan, K. G. Neoh, E. T. Kang, *J. Phys. Chem. C* **114** (2010) 12742
12. C. P. Tien, H. S. Teng, *J. Power Sources* **195** (2010) 2414
13. J. J. Liang, Y. Wang, Y. Huang, Y. F. Ma, Z. F. Liu, J. M. Cai, C. Zhang, H. Gao, Y. Chen, *Carbon* **47** (2009) 922
14. S. Park, N. Mohanty, J. W. Suk, A. Nagaraja, J. An, R. D. Piner, W. Cai, D. R. Dreyer, V. Berry, R. S. Ruoff, *Adv. Mater*. **22** (2010) 1736
15. T. K. Das, S. Prusty, *Polym. – Plast. Technol. Eng*. **52** (2013) 319
16. K. Hu, D. D. Kulkarni, I. Choi, V. V. Tsukruk, *Prog. Polym. Sci*. **39** (2014) 1934
17. J. P. Fouassier, J. Lalevée, *Photoinitiators for Polymer Synthesis: Scope, Reactivity and Efficiency*, Wiley–VCH, Weinheim, 2012
18. N. B. Cramer, J. W. Stansbury, C. N. Bowman, *J. Dent. Res*. **90** (2011) 402
19. E. C. Buruiana, F. Jitaru, A. Matei, M. Dinescu, T. Buruiana, *Eur. Polym. J*. **48** (2012) 1976
20. I. Sideridou, V. Tserki, G. Papanastasiou, *Biomaterials* **23** (2002) 1819
21. J. F. G. A. Jansen, A. Dias, M. Dorschu, B. Coussens, *Polym. Prepr*. **42** (2001) 769
22. M. A. Tasdelen, N. Moszner, Y. Yagci, *Polym. Bull*. **63** (2009) 173
23. Y. L. Zhang, Q. D. Chen, H. Xia, H. B. Sun, *Nano Today* **5** (2010) 435
24. A. Ovsianikov, A. Deiwick, S. Van Vlierberghe, M. Pflaum, M. Wilhelmi, P. Dubruel, B. Chichkov, *Materials* **4** (2011) 288
25. S. D. Gittard, R. J. Narayan, *Expert Rev. Med. Devices* **7** (2010) 343
26. M. Farsari, M. Vamvakaki, B. N. Chichkov, *J. Opt. (Bristol, U.K.)* **12** (2010) 124001
27. A. Ovsianikov, M. Malinauskas, S. Schlie, B. Chichkov, S. Gittard, R. Narayan, M. Löbler, K. Sternberg, K. P. Schmitz, A. Haverich, *Acta Biomater*. **7** (2011) 967
28. E. C. Buruiana, F. Jitaru, A. Matei, M. Dinescu, T. Buruiana, *Soft Mater*. **11** (2013) 165

29. S. Yamashita, Y. Saito, J. H. Choi, *Carbon nanotubes and graphene for photonic applications*, Woodhead Publishing, Oxford, 2013
30. T. Hasan, Z. Sun, F. Wang, F. Bonaccorso, P. H. Tan, A. G. Rozhin, A. C. Ferrari, *Adv. Mater*. **21** (2009) 3874
31. M. Oubaha, A. Kavanagh, A. Gorin, G. Bickauskaite, R. Byrne, M. Farsari, R. Winfield, D. Diamond, C. McDonagh, R. Copperwhite, *J. Mater. Chem*. **22** (2012) 10552
32. G. Temel, N. Karaca, N. Arsu, *J. Polym. Sci., A: Polym. Chem.* **48** (2010) 5306
33. W. S. Hummers, R. E. Offeman, *J. Am. Chem. Soc*. **80** (1958) 1339
34. N. P. Patel, M. A. Hunt, S. Lin-Gibson, S. Bencherif, R. J. Spontak, *J. Membrane Sci*. **251** (2005) 51
35. E. C. Buruiana, T. Buruiana, V. Melinte, M. Zamfir, A. Colceriu, M. Moldovan, *J. Polym. Sci., A: Polym. Chem*. **45** (2007) 1956
36. J. Su, M. H. Cao, L. Ren, C. Hu, *J. Phys. Chem. C* **115** (2011) 14469
37. M. Zhang, M. Jia, Y. Jin, *Appl. Surf. Sci*. **261** (2012) 298
38. Z. L. Wang, D. Wu, Y. Huang, Z. Wu, L. Wang, X. Zhang, *Chem. Commun*. **48** (2012) 976
39. E. C. Buruiana, A. Chibac, T. Buruiana, V. Melinte, L. Balan, *J. Nanopart. Res.* **15** (2013) 1335
40. M. Sangermano, S. Marchi, L. Valentini, S. B. Bon, P. Fabbri, *Macromol. Mater. Eng*. **296** (2011) 401
41. M. Martin-Gallego, R. Verdejo, M. A. Lopez-Manchado, M. Sangermano, *Polymer* **52**
42. L. Zhang, J. Liang, Y. Huang, Y. Ma, Y. Wang, Y. Chen, *Carbon* **47** (2009) 3365
43. B. D. Cullity, *Elements of X-Ray Diffraction*, Addison-Wesley Publishing, Reading, MA, 1978
44. X. Zhao, Q. Zhang, D. Chen, P. Lu, *Macromolecules* **43** (2010) 2357.